Commercial carbon composition resistors as dynamic stress gauges in difficult environments

Cite as: Review of Scientific Instruments **62**, 2218 (1991); https://doi.org/10.1063/1.1142340
Submitted: 01 April 1991 . Accepted: 03 June 1991 . Published Online: 09 September 1998

Michael J. Ginsberg, and Blaine W Asay

Commercial carbon composition resistors as dynamic stress gauges in difficult environments

Michael J. Ginsberg and Blaine W Asay
Explosives Applications (M-8), Los Alamos National Laboratory, MS J960, Los Alamos, New Mexico 87545

(Received 1 April 1991; accepted for publication 3 June 1991)

Commercial carbon composition resistors have been used as gauges to make dynamic stress measurements in homogeneous and heterogeneous reactive and inert materials. Initial loading was provided by plane wave lenses or shaped charge jets. A series of gas gun and aquarium experiments has been conducted to characterize the behavior of the gauges. Calibrations up to about 14 GPa for nominal 470 Ω resistors and 17 GPa for nominal 4700 Ω resistors are presented. The accuracy of the carbon resistor gauges is limited by response time considerations when submicrosecond rise times are encountered, and there is hysteresis during release. The gauge-to-gauge reproducibility appears to be adequate, and they survive in situations where no other stress transducer has been successfully used, such as in reacting beds of large-particle gun propellants.

I. INTRODUCTION

Making time-resolved stress measurements *in situ* in difficult environments is not a simple task. Examples of such difficult environments are dynamically loaded composite, particulate, and reactive materials, multidimensional and reactive flows, and combinations of these materials and conditions. Conventional piezoresistant gauges, such as those using manganin as the active element, are more useful in one-dimensional flow fields in homogeneous materials.

However, we sometimes need time-resolved measurements of the amplitude and duration of waves propagating in these materials. The stress range of interest is ~0.1 GPa to above 10 GPa. Although well-insulated manganin foil gauges have worked well in one-dimensional reactive flows in somewhat heterogeneous explosives (less than 10% porosity), gauges fabricated from foils or films do not survive in more heterogeneous materials, especially when there is also chemical reaction. Local particle velocity gradients apparently cause early failure of the gauge and useful data are rarely obtained.

When the gauge is placed outside the flow, in a "back-surface" configuration, survivability is improved and the wave front is smoothed, but the dynamic properties of the gauge encapsulant and the material of interest must then be known beforehand because of the impedance mismatch problem. Some investigators have assumed perfect impedance matches, but this is rarely obtainable in actuality.

Uncertainties in calibration accuracy of ~2% have been quoted for manganin gauges in one-dimensional flow in homogeneous materials.[1] We would like to attain this level of accuracy in the more difficult environments, but if the transducer does not survive beyond the wave arrival, the degree of accuracy (and precision) is irrelevant. After several experiments in which we attempted to use well-armored manganin gauges in beds of large particles, another means of making the measurements had to be found, even if some accuracy had to be sacrificed for survivability.

Building on the work of others, we have modified commercial $\frac{1}{8}$ W carbon composition resistors so that they have acceptable survivability in extremely hostile dynamically loaded environments. This article describes our work to date including measurements in heterogeneous and homogeneous materials, inert and reactive materials, and one-dimensional and multidimensional flow fields.

II. BACKGROUND

Watson[2] was the first to show that the resistance of $\frac{1}{8}$ W carbon composition resistors appears to decrease in a reproducible manner when they are dynamically loaded at ≈1–7 GPa. His calibration curve related the final resistance value of nominal 470 Ω (actual 452±0.5) resistors to peak stress, and he found that the curve consisted of two distinct, nearly linear regions linked by a curved segment between 1.5 and 3 GPa. The sensitivity of the carbon resistor gauges (CRGs) above 3 GPa was much less than at 1.5 GPa and below. No attempt was made to consider the release portion of the time-resolved data; only peak stress data were used in the calibration.

Stankiewicz and White[3] investigated the resistance change of nominal 220 Ω, $\frac{1}{8}$ W resistors under hydrostatic pressure at three different temperatures (4.2, 77, and 295 K). Their pressure coefficients of resistance varied with initial temperature. We will discuss some evidence regarding temperature effects during dynamic compression.

Austing, Tullis, and Johnson[4] studied the detonation characteristics of very low density explosives and used CRGs embedded in polymer blocks in contact with the explosive. They also did some calibration experiments and proposed a calibration curve consisting of two linear portions joined at ~3 GPa.

Scholz[5] constructed transducers with 470 Ω carbon resistors as the active elements to measure pressures generated in boreholes during explosive mining operations. The rise time associated with these events was approximately 10^{-3} s, significantly longer than that encountered

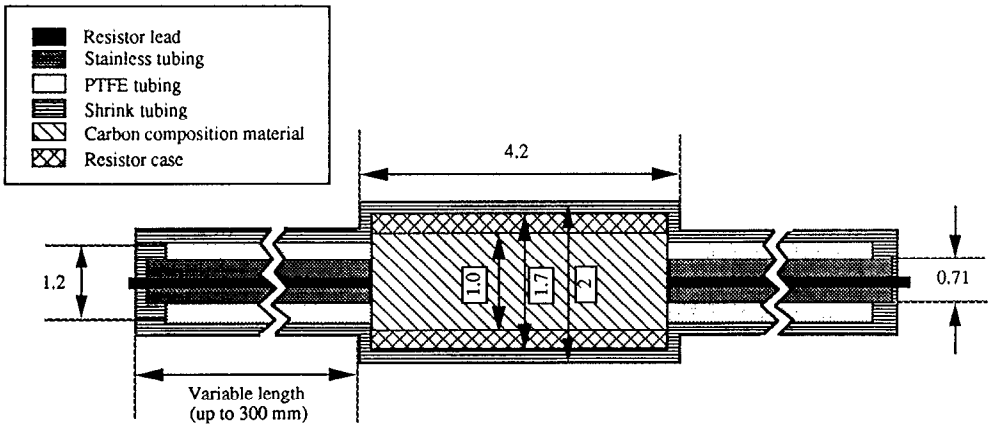

FIG. 1. Schematic of carbon composition resistor modified for stress gauge application. Dimensions are in millimeters.

in shock wave experiments. He compared Watson's[2] shock wave calibration experiments, those of Hollenberg,[6] the static work of Stankiewicz and White,[3] and his own calibration by means of a drop hammer, which produces well-characterized stress pulses with rise times of approximately 10^{-3} s. The static calibration agreed very well with the millisecond time-scale calibration up to 1.1 GPa, the highest value of stress attained in the experiments. Also, the transition from static and millisecond-range calibration experiments to shock wave results above 1 GPa was smooth, suggesting that rate effects do not greatly influence gauge response, at least in this stress range.

Hollenberg[6] did extensive calibration experiments on 47, 470, and 4700 Ω resistors (nominal values). He suggested that the 4700 Ω CRGs were not saturated until the stress was over 25 GPa, possibly extending the useful range of these devices. In addition, he obtained several Hugoniot curves and he tried to use the CRGs in detonating nitromethane. He explains that this failed because the conductive detonation products shunted the gauge, giving an incorrect voltage change. In a subsequent paper,[7] Hollenberg made several back-surface measurements using CRGs embedded in polymethylmethacrylate (PMMA) in contact with PETN explosive.

We decided that, if properly constructed and insulated, transducers with $\frac{1}{8}$ W CRGs as the pressure-sensing elements might survive reactive and heterogeneous environments. We modified the resistors as described in the next section, and exposed the CRGs to a wide range of materials and flow conditions.

III. HARDWARE

A. Gauges

Standard $\frac{1}{8}$ W carbon composition resistors made by the Allen-Bradley Co. were used for this study. High-stress (> 60 kbar or 6 GPa) and low-stress applications called for resistors with nominal resistance values of 4700 and 470 Ω, respectively. Several different gauge construction, protection, and placement methods were tried before a reliable technique was found. Figure 1 is a schematic of the gauge arrangement that proved most successful. The stainless steel hypodermic tubing is used as a resistor-lead extension. This is a more rugged assembly than one obtained when extension leads are soldered to the resistor. Polytetrafluoroethylene (PTFE) and heat-shrinkable tubing insulate the gauge from surrounding material. Gauges must be insulated because reactive fronts usually are also conductive and can short out an unprotected gauge. A gauge may be used in the linear configuration, as shown, but typically, the leads are bent at an angle and are then brought out of the target through the side downstream from the flow. All connections close to but outside the shot assembly must usually be fully insulated to avoid a short circuit caused by expanding reaction products.

B. Related systems

Figure 2 is a schematic of the simple circuit used to find gauge resistance as a function of time, $R(t)$. In terms of the initial gauge resistance $R_g(t = 0)$, the termination resistance R_t, the supply voltage E_0, and the viewing resistance R_v, we define a constant

$$C=\frac{E_0}{R_v[1/R_g(t=0) + (1/R_t)] + 1}. \tag{1}$$

The difference between the initial and final voltage is ΔV, where

$$R_g(t)=\{(1/R_v)[E_0/(C-\Delta V) - 1] - 1/R_t\}^{-1}. \tag{2}$$

Figure 3 diagrams the circuit board used during the experiments. The cables to the gauges are 3.6 m long, and the power and scope cables are 15.2 m long. R_v is nominally 50 Ω. Each capacitor packet contains four capacitors of 6.8, 1.0, 0.1, and 0.01 μF, respectively. These maintain constant voltage at the gauge for the duration of the measurement period. During an analysis of the entire circuit, a

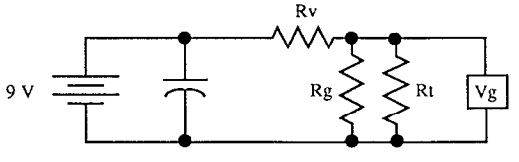

FIG. 2. Circuit for determining gauge resistance as a function of time during dynamic loading.

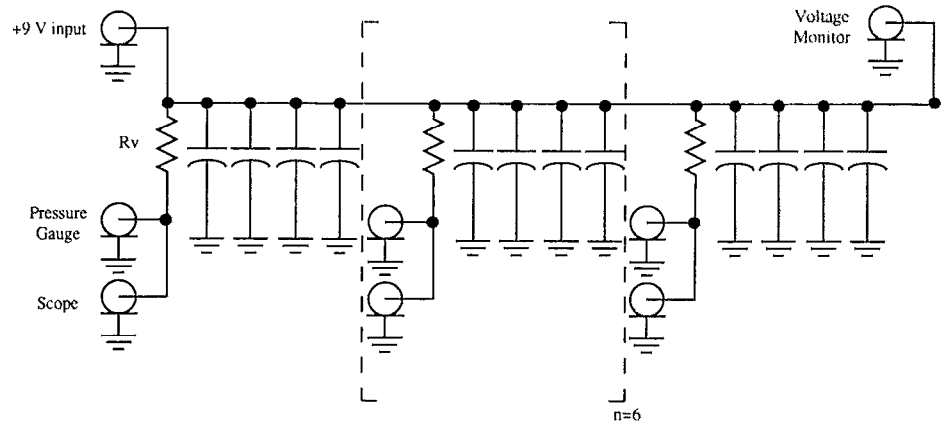

FIG. 3. Schematic of circuit used to measure resistance charge of eight carbon resistor gauges simultaneously.

field effect transistor (FET) was used to switch a 5 Ω resistor into a parallel position with a 470 Ω resistor to simulate a rapid change in stress. A rise time of approximately 220 ns was noted, well within our requirements, with no ringing at the top of the initial signal.

Circuit analysis examined whether the nonlinearity of the calibration curve caused increased uncertainty in the final $P(t)$, where P is the longitudinal stress. Figure 4 plots $V(R/R_0)$ with a plot of $V(P)$, where V is the voltage measured at a given R/R_0. The relationship between P and measured voltage is nearly linear, which demonstrates that the circuit used tends to counteract the effects of the nonlinear relationship between P and R/R_0.

The data have been recorded with LeCroy 8818 and 8828 digitizers, 6108 amplifiers, and 9400 digital oscilloscopes.

IV. EXPERIMENTS

A. Calibration experiments

We have completed a series of light-gas gun experiments designed to serve three purposes. First, we compared the peak stress versus resistance change data obtained from well-defined flat-topped input waves with previously published calibration curves. Second, we investigated the detailed time-resolved response of the gauges (including the release behavior) and compared the response to known wave profiles. Third, we contrasted the behavior of the gauges in one-dimensional flow with their behavior in spherically divergent flow. We also used "aquarium" tests[8,9] to determine peak stress calibration points. Figures 5 and 6 show calibration curves for nominally 470 Ω resistors based on these data. The equation for the fit is

$$P(\mathrm{GPa}) = 7.001 - 4.345(R/R_0) + 0.364(R_0/R) - 8.40\exp -(R/R_0). \quad (3)$$

The two major issues in these gas gun experiments were the accuracy and reproducibility of the gauges. During time-resolved measurements of stress histories, a very accurate gauge would register a stress value that is essentially correct during the passage of the wave (except in the shock front, if it is a classical discontinuity). Therefore, accuracy can be affected in the gauge if time is inadequate for the rate of change in the stress in the wave profile.

Figure 7 is two measured wave profiles obtained with 470 Ω carbon resistors from an aluminum-on-aluminum

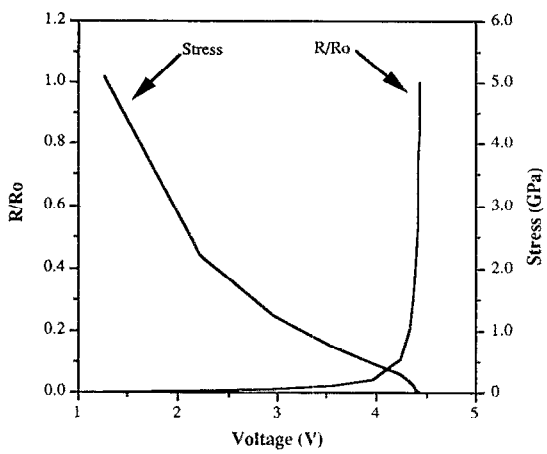

FIG. 4. Comparison of resistance change and stress as a function of voltage for a 4700 Ω resistor.

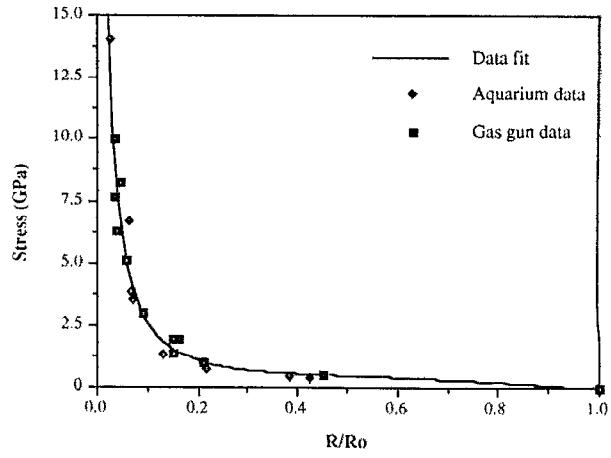

FIG. 5. Calibration curve for carbon resistor gauges with nominally 470 Ω resistance.

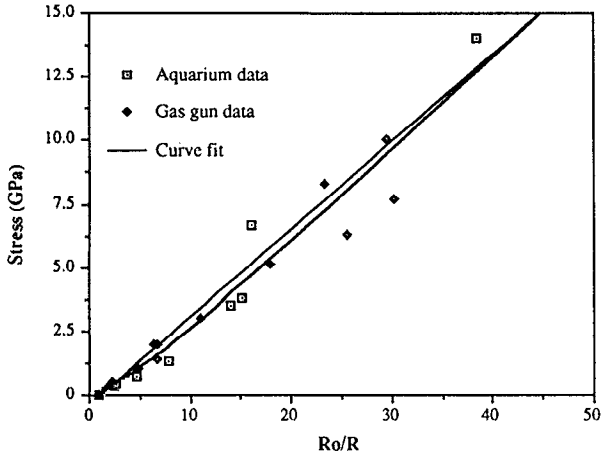

FIG. 6. Another representation of the 470 Ω calibration data.

symmetrical impact experiment. The projectile velocity was 0.256 km/s. The reproducibility is very good. However, the time needed for the gauges to equilibrate with the wave causes the steps seen on the front of the wave. The characteristic rise time of the carbon resistor gauges seems to be about 1 μs in this shock velocity regime. At higher shock velocity (and stress) the rise time can be substantially less.[7] These records show a three-step rise to the peak, followed by a falling ramp and the arrival of the release wave, with a subsequent return to the original voltage level. Other gauges, usually after exposure to a higher stress level, have returned to a voltage level just under the base line, signifying a slightly positive (greater than the original gauge resistance) residual resistance. This effect probably arises from damage to the resistor caused by the wave, an increase in temperature, or a combination of the two.

The predicted waveform consists of a sharp rise, a flat top, and the arrival of the release wave 3.75 μs after the shock. Comparing the two gauge records with the predicted shape points out the following problems. First, the

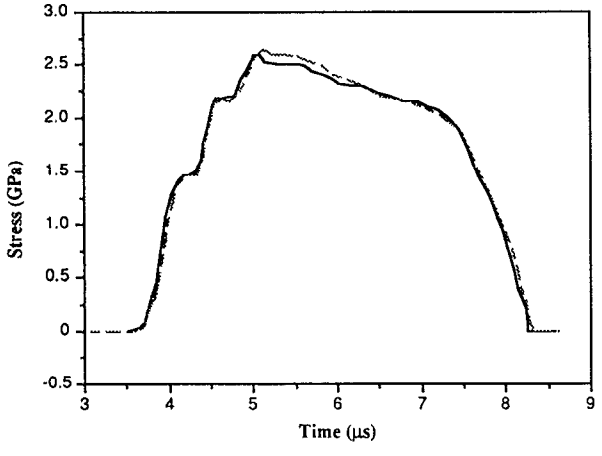

FIG. 7. Two carbon resistor gauge records from a gas gun experiment.

gauges cannot respond accurately to waves with rise times less than about 1 μs, if there is an impedance mismatch between the gauge and the surrounding material. Under the best circumstances, the gauge equilibrates with the surrounding material without ringing up (perfect impedance match) and the maximum velocity in the stress-sensitive carbon composition portion of the resistor (about 1 mm diameter) would be about 5 mm/μs; thus, the best rise time we could ever expect would be about 200 ns. Hollenberg[7] reports rise times of 125 ns for resistors embedded in PMMA, so our predictions may be overly conservative. Figure 7 shows that each transit through the resistor requires less time than the one before because the shock velocity through the gauge increases with compression, and the diameter of the resistor is reduced.

The stress levels of both gauges decrease after the peaks at approximately 5 μs because of release waves originating at the epoxy-filled grooves in which the gauges are embedded. These ramps were not seen when the gauges were embedded in PMMA targets, and records from our later experiments with high-impedance targets and single gauges did not include this feature.

The release wave originating at the back of the target was predicted by a one-dimensional wave propagation code to arrive at the gauges 3.75 μs from impact. The measured time of arrival was between 3.50 and 3.75 μs from impact. The release wave appears to become steeper with time, suggesting that the gauge's response to release is affected by how fast the gauge recovers from deformation during compression. Hysteresis during release has been reported for every other piezoresistant gauge in use today, so this behavior is not unexpected.

We attempted to calibrate the release portion of the gauge response with step-release experiments. In these experiments, the target was backed by a low-impedance foam so that the initial release would not be to zero stress, but rather to some intermediate state dictated by the shock properties of the foam and the release adiabat of the PMMA. We found, however, that the carbon resistor gauge could not respond quickly enough to the step in the release wave (Fig. 8). This behavior probably relates to hysteresis effects but we have too few data to offer a complete explanation. We recently published an erroneous version of Fig. 8 that caused the release behavior of the carbon resistor gauge to seem less accurate than it is.[10] The problem was caused by an error in the relative positions of the carbon resistors and manganin stress gauges in a target. Figure 8 has been corrected and now shows that the release behavior of the carbon resistor gauge is qualitatively correct but cannot be used to obtain quantitative details of the release behavior of the material in which they are embedded. The gauge is not in exact stress equilibrium with the surrounding material during release (or compression) in this time regime. The observation that the resistance returns to the original value after complete release suggests that no serious temperature effects occur during compression or release.

We performed one experiment in which we struck the target with a round-nosed (50.8 mm radius) aluminum

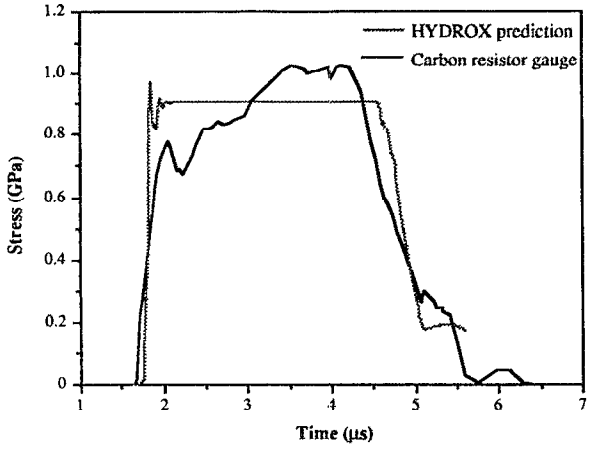

FIG. 8. Comparison between carbon resistor gauge record and HYDROX code prediction for step-release experiment.

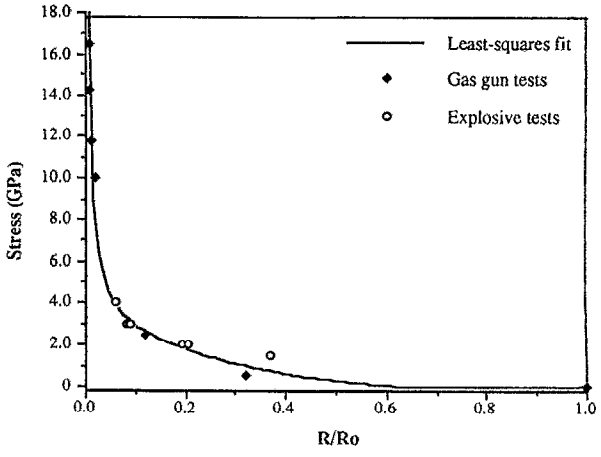

FIG. 10. Calibration curve for carbon resistor gauges using nominally 4700 Ω resistors.

projectile instead of a flat flyer plate. The target was fabricated from a castable epoxy-aluminum powder mixture and the gauges were placed at 9.5, 19.0, and 28.6 mm from the front surface. In a previous experiment,[11] strain-compensated carbon film gauges had shown the longitudinal stress to be 1.61, 1.31, and 0.76 GPa at the three gauge locations when the projectile velocity was 0.75 km/s. The measured terminal projectile velocity during our experiment was 0.72 km/s. We have accounted for the projectile velocity difference by a simple linear correction in the stress. Figure 9 shows our best 470 Ω calibration curve fitted to the set of points obtained from the one-dimensional strain gas-gun experiments and the aquarium test. The three data points shown are from the divergent flow experiment. Agreement between the points obtained during the divergent flow experiment is very good. Apparently, the tangential strain (as much as 10% in the original experiment) does not affect the gauges or it does not couple into the gauges. More data are required to demonstrate this agreement over the useful range of the gauges. We expect to perform more divergent flow experiments, in both spherical and cylindrical geometries.

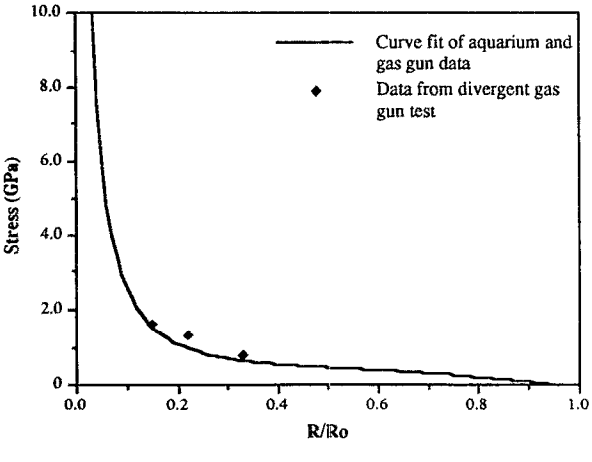

FIG. 9. Comparison of gauge response when subjected to planar and spherically divergent flow. The line is fitted to all the 470 Ω one-dimensional data. The points are from the spherically divergent flow experiment.

Figure 10 is a calibration curve for nominal 4700 Ω (±5%) resistors. The curve is fitted to data obtained from six gas gun experiments. The equation for this curve is

$$P(\text{GPa}) = -13.846 + 7.70(R/R_0) + 0.1006(R_0/R) + (16.604)\exp -(R/R_0). \quad (4)$$

The other six points were obtained from experiments done with a calibrated explosive system.[12] We have not specifically investigated either the divergent-flow response or the release behavior of 4700 Ω gauges, but we have assumed, pending further experiments, no basic qualitative difference between the 470 and 4700 Ω resistors. We have tended to use 4700 Ω resistors when we expect higher stress levels—above 5 to 7 GPa—and, to be conservative, when we cannot estimate the maximum stress level to be seen by the gauge.

B. Jet penetration experiments (cylindrical divergent flow)

These experiments and results have been described in detail elsewhere.[13] We include them here as a complete account of our work with CRGs. We did three sets of experiments in which light antitank weapon (LAW) shaped-charge jets were fired into tubes filled separately with water, rice, and a granular gun propellant, designated M30A1. These were designed to show how the stress field varied during penetration through nonreactive homogeneous, nonreactive heterogeneous, and reactive heterogeneous materials. The detonation behavior of M30A1 has been described elsewhere.[10] The LAW jets had tip velocities of 8 mm/μs. The jet diameters were approximately 3 mm. Figure 11 is a schematic of the experimental shot configuration for the experiments using propellant and rice. The experiment with water had two tiers of gauges

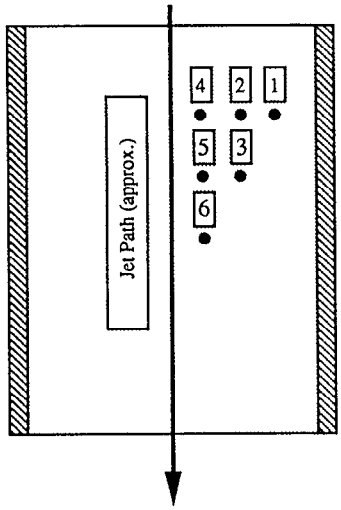

FIG. 11. Schematic of jet interaction test configuration used during the rice and propellant experiments. Dark circles show relative positions of the carbon resistor gauges. Numbers refer to gauge positions referenced in the following figures.

with three gauges at each level. The actual tube dimensions for the three sets of experiments differed slightly.

Figure 12 shows the $P(t)$ data resulting from the penetration of water by the LAW in two experiments designed to be identical. The figure shows the radial stress profiles at

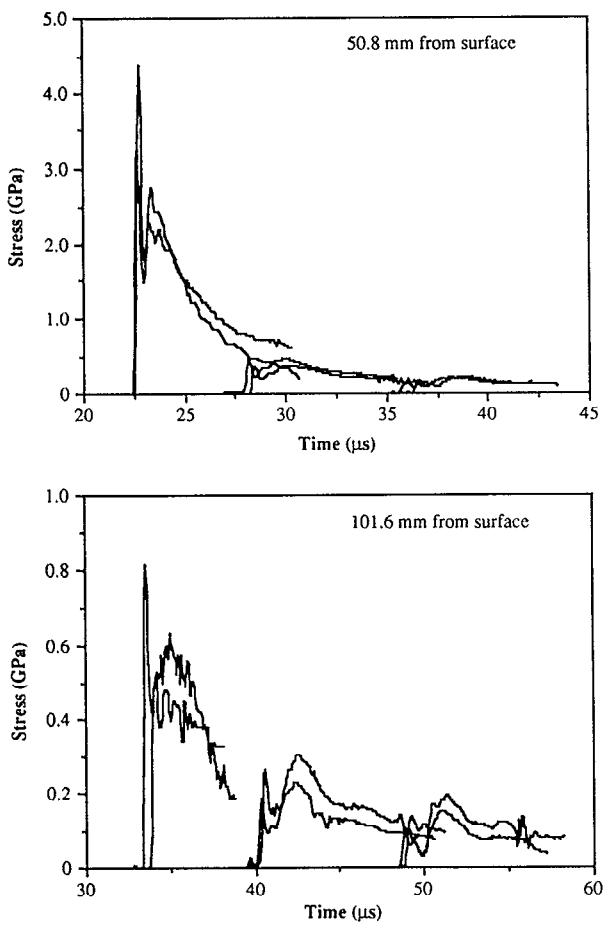

FIG. 12. Stress-time histories obtained with carbon resistor gauges during jet penetration of water. Three gauges were placed at each level shown in the figure.

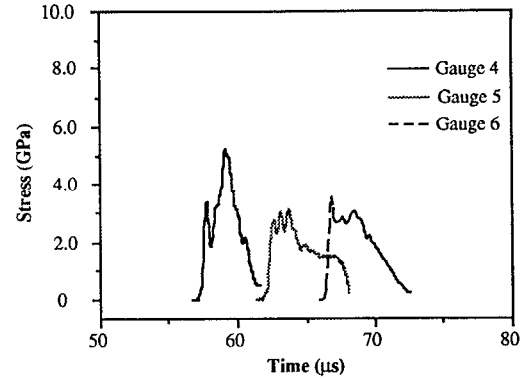

FIG. 13. Data from gauges 4, 5, and 6 for a LAW penetrating rice. Gauge positions indicated in Fig. 11.

two different axial positions. The two sets of gauges were 50.8 m and 101.6 mm axially from the top of the tube and the three gauges were 12.7, 31.8, and 50.4 mm from the jet axis, respectively. The agreement in the stress records between the shots is very good.

Figure 13 shows the data from the LAW penetration of rice. The stress levels are somewhat lower than for the propellant described below. The response of gauges 1, 2, and 3 were below our detection limits. The decrease in stress with radial distance appears to be very large, which is the reason that porous materials are used as shock attenuators.

The three propellant penetration experiments used M30A1 as the propellant, with 4700 Ω gauges for two experiments and 470 Ω gauges for the third. They were designed to be identical in every other detail to verify the gauge reproducibility. Figures 14 and 15 show the data from these experiments. Large differences are evident in both time and magnitude. The gauge records indicate totally different reaction and wave propagation behavior in apparently identical experiments. This is an interesting and somewhat disturbing (but not necessarily surprising) result, which is discussed in some detail in Ref. 13, and is probably caused by differences in the configuration of the jet tips or other parts of the jets. However, these data confirm that, with proper care, measurements can be made in the near-field regions of jet penetration. In shot no. C-6105, no power was applied to gauge 6 to examine the electrical effects of the reaction front on the gauges. A small response, corresponding to approximately 0.01 GPa, was noted after passage of the front.

C. Plane wave (one-dimensional strain) experiments

In addition to the gas gun calibration experiments described in Sec. IV A, we investigated two other plane flow situations, but in heterogeneous rather than homogeneous materials. For the nonreactive case, we chose glass beads, and for the reactive case, a granular gun propellant. The glass beads represented a system in which we could vary the particle (bead) size and attempt to determine the effect of size and porosity on wave propagation. A schematic

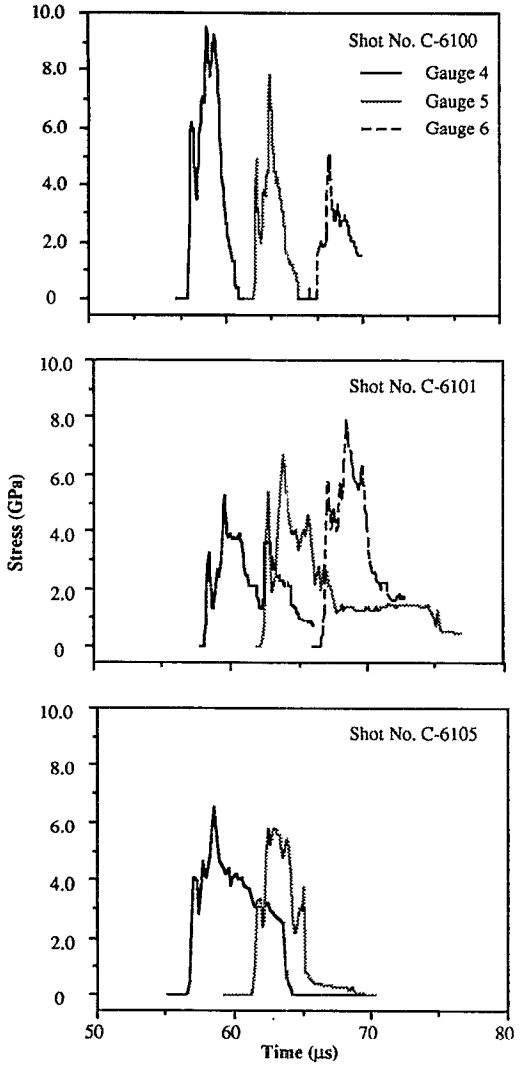

FIG. 14. Data from gauges 4, 5, and 6 for a LAW penetrating propellant. Gauge positions indicated on Fig. 11.

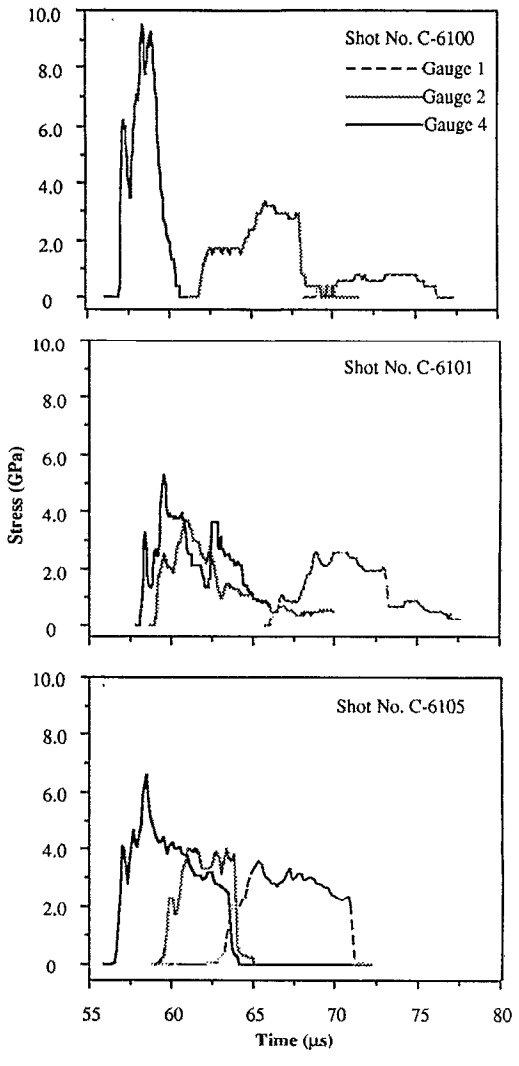

FIG. 15. Data from gauges 1, 2, and 4 for a LAW penetrating propellant. Gauge positions indicated in Fig. 11.

drawing of these experiments is shown in Fig. 16. The soda-lime glass beads used in this particular experiment were spherical and the average diameter was 3 mm. The density was 2.56 ± 0.09 g/cm^3 and the porosity of the bed was 0.41 ± 0.03.

Carbon resistor gauges (three at each level) were placed at two different axial positions 12.5 mm apart. The assembly was dynamically loaded with a P-040 plane wave lens. The stress-time records from the gauges are shown in Fig. 17. The peak stress measured by the upper gauges was 17.7 ± 1.8 GPa and by the lower gauges, 10.8 ± 1.8 GPa. We believe that the stress we are measuring in these experiments is the intragranular stress, defined as the average axial compressive force per unit radial cross-sectional area of the solids in the porous bed, as discussed by Kuo, Moore, and Yang[14] and by Coyne and Elban[15] and given in this case by

$$T_i = \frac{F}{A(1-\phi_{\mathrm{AVG}})}, \tag{5}$$

where F is the force applied to the bed, which has overall area A, and ϕ_{AVG} is the average fractional porosity. The variability in the response could very well reflect the actual local stress level at the different gauge locations, which

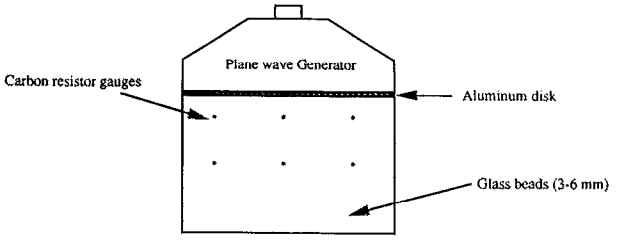

FIG. 16. Experimental arrangement for studying wave propagation in glass beads.

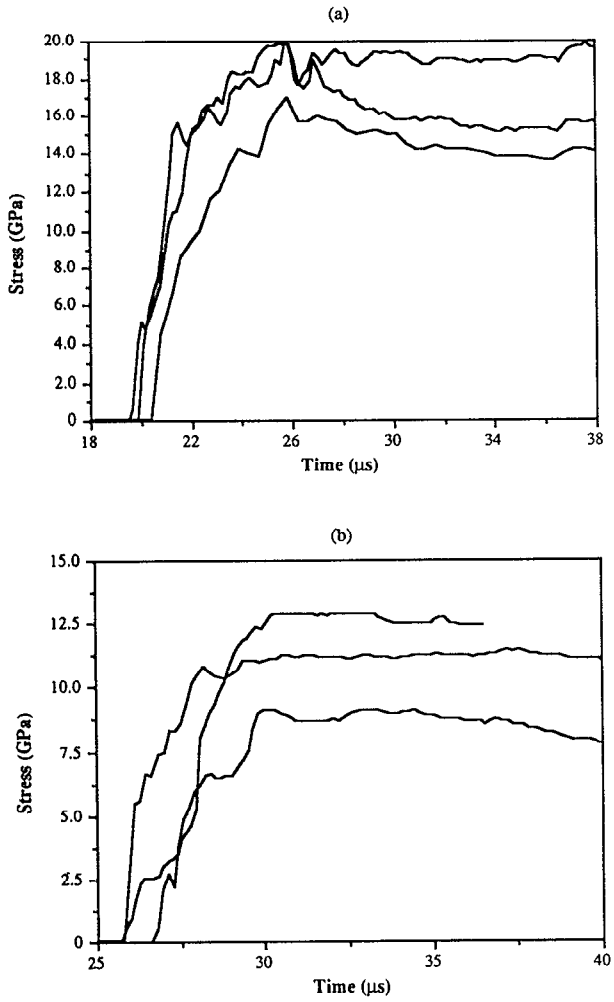

FIG. 17. Stress-time data from shot no. C-6169, 3 mm glass bead loaded with a P-040 plane wave generator. Gauges 1, 2, and 3 were located 17.2 mm from the explosive interface, and gauges 4, 5, and 6 were located 30 mm from the interface.

would be affected by the configuration of the beads surrounding each gauge. The records suggest that T_i attenuates by about 0.2 GPa/mm between the two gauge levels. The calculated maximum amount of time that the gauges were in an area of one-dimensional flow is about 20 μs. It seems, therefore, that we can accept as valid at least the first 15 μs of these records. However, we have no release calibration and Fig. 17 inadequately describes the release behavior of the bed of beads. We expect that the actual rarefaction wave would be steeper than that shown in the figure. At present, we have no other way of making this type of measurement, so we suggest that this level of reproducibility is acceptable.

We continued this line of investigation by placing CRGs in a bed of granular M-10 gun propellant and dynamically loading the bed with an explosive plane wave generator and 50.8 mm of TNT. A 3.25-mm-thick sheet of PMMA was placed between the TNT and the propellant. The four gauges were located 50.8 mm below the PMMA-propellant interface. We were concerned about the possibility that conducting reaction products might affect the

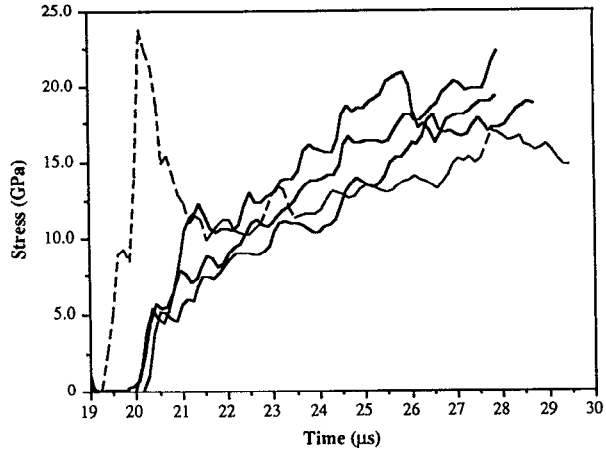

FIG. 18. Gauge records from plane flow experiment in M-10 propellant. CRG1 was not electrically insulated.

gauge response, so we placed an uninsulated gauge (CRG-1) at the same plane as the other three conventionally insulated (see Fig. 1) gauges so that we could look for differences in behavior.

The results are shown in Fig. 18. Clearly, there is a difference between the insulated gauges and the uninsulated gauge (CRG-1). The insulated gauges show a fast-rising wave followed by a slower increase in stress, probably caused by a reactive buildup behind the shock. The wave form resembles those seen in, for example, porous conventional explosives during buildup to detonation.[16] The uninsulated gauge exhibits a large decrease of resistance, possibly caused by conductive reaction products that are leading the shock through the pores in the propellant. Precursors of reacted material have also been seen in conventional porous explosives.[17,18] After about 2.5 μs, the conductive part of the front apparently passes the gauge, and the remaining signal, which agrees reasonably well with the signal from the insulated gauges, is from the stress-induced resistance change. The results from this experiment suggest strongly that the insulation scheme normally used on these CRGs is sufficient to protect them from reaction products in reactive flow situations long enough for us to make our measurements.

V. DISCUSSION

A. Calibration results

The most extensive calibration data presented so far have been those of Hollenberg.[6] Our calibration results (Figs. 5 and 10) differ significantly from Hollenberg's beginning at 7 GPa for the 4700 Ω resistors and, to a lesser extent, at >5 GPa for the 470 Ω resistors. Our recommended upper limit to the useful range of the 470 Ω resistors is 5 GPa, so this presents no problem, even though the 4700 Ω data do not agree. We believe that about 16 GPa represents a good estimate of the upper range of those resistors. In extrapolating beyond this, as we did for the glass bead experiments, caution should be used.

TABLE I. Summary of flow/material combinations and applicability of gauges.

Flow	Material	Manganin gauge	Resistor gauge	Relative difficulty	Example
Planar nonreactive	Homogeneous	Yes	Yes	Low	Gas gun
Planar reactive	Homogeneous	Yes	No	Medium	Nitromethane
Divergent nonreactive	Homogeneous	Yes	Yes	Medium	Jet-water
Divergent reactive	Homogeneous	No	No	Medium	Jet-nitromethane
Planar nonreactive	Heterogeneous	No	Yes	Medium	Glass beads
Planar reactive	Heterogeneous	No	Yes	High	P-40/propellant
Divergent nonreactive	Heterogeneous	No	Yes	High	Jet/rice
Divergent reactive	Heterogeneous	No	Yes	High	Jet/propellant

Hollenberg employed the following method to calibrate his CRGs. The gauges were placed in water in a PMMA tube at a known distance from the flat face of a cylinder of 60 wt. % RDX/40 wt. % TNT (composition B). The explosive was detonated at the opposite end, and the time of arrival of the shock wave at each of the CRGs was measured, along with the changes in resistance of each gauge. A large number of these time-of-arrival measurements were made, and from them, a shock-velocity-versus-position curve was generated by fitting and differentiation.

Given the shock velocity, existing Hugoniot equation-of-state data were used to calculate the particle velocity and, ultimately, the stress as a function of distance from the explosive face. The change in resistance of the CRGs at known distances was then correlated to the stress at that distance, producing the desired calibration curve.

If we compare the stress-distance curve obtained by Hollenberg using comp B and water with a stress-distance curve obtained similarly using Pentolite explosive and water,[8,9] we see that the interface stress obtained by Hollenberg is smaller than that obtained in the other experiment. The Chapman–Jouguet (CJ) pressure of comp B is larger than that of Pentolite, so this seems unlikely and could be a source of error. Because we know the conditions obtained during the gas gun experiments with great accuracy (better than 1% in projectile velocity), we believe that our calibration curves are more descriptive of the actual gauge behavior in the range of usefulness for each type. The agreement between our gas gun and aquarium results for the 470 Ω gauges adds weight to this observation.

We have not been able to calibrate the CRGs during release. We believe, however, that their considerable hysteresis occurs because they cannot recover quickly from the strain experienced during compressive loading. This was also discussed in Ref. 19. We have not yet attempted to quantify the reloading behavior, but we have seen instances where the gauges respond to multiple stress waves. Further research is needed here, as well as a greater understanding of the gauge response during release.

B. Other experiments

Table I lists the eight flow field and material combinations in which we might wish to make dynamic stress measurements. The columns labeled "Manganin gauge" and "Resistor gauge" contain information regarding whether or not (to the best of our knowledge) measurements have been made under the described conditions with conventional piezoresistant foil gauges (manganin in only an example) or with CRGs. The relative difficulty of each measurement type is meant to be an internal comparison. In general, heterogeneity, reactivity, and divergence add to the difficulty, with heterogeneity being the greatest problem. In addition, other factors are involved besides flow field and material (peak stress, for example). In this article, we have described measurements in six of the eight flow field-material combinations with CRGs.

The jet-water interaction experiments demonstrated the reproducibility of the gauges in a divergent flow field in which we might not expect coupling of tangential strain into the gauges, but some bending should take place. These experiments were straightforward and, for situations where the time resolution of the CRGs is not a limiting factor, this represents a useful application. It is possible, however, that in this type of experiment, a conventional foil gauge might be the transducer of choice, depending on the specific requirements of the experimenter.

Performing well in the jet-rice and jet-propellant interaction experiments would be a severe problem for conventional piezoresistant gauges. We believe that the carbon resistor gauge is the best gauge for these applications in terms of survivability and data return. In the reactive case (jet propellant), growth or decay of reaction could be clearly seen in the gauge records The plane-wave-loaded equivalents to these experiments, which were done with glass beads and a granular gun propellant with grain size approximately that of the CRGs, would have been equally difficult to perform with conventional piezoresistant gauges. The reactive case (the gun propellant) may actually present a less severe challenge than the glass beads because we are measuring in a dense-gas/partially reacted grain mixture that could be less heterogeneous than the beads. Although more data are needed to understand the behavior of the gauges in these materials, the CRG now offers the best possibility of direct study of stress wave propagation in materials that are as grossly heterogeneous as glass beads and gun propellants.

C. Theoretical work

Gauge behavior, as represented by inclusions of various shapes in matrices of various properties, has been studied by many investigators.[20–24] These authors all considered and analyzed the response of piezoresistant gauges embedded in homogeneous matrices. Also of interest to the carbon resistor case is the discussion by Wilson and coworkers,[19] who consider a cylindrical inclusion surrounded by material 1 embedded in a matrix of material 2. From these analyses and from basic stress wave physics, the limitations and problems encountered during tests with CRGs are not unique. The size of the gauge affects the response, as do impedance mismatches. The strain state in the gauge is not the same as that in the matrix. Improved understanding of these complex phenomena should follow further experimentation and analysis.

ACKNOWLEDGMENTS

This work was supported by the DA/DOE Research Program, and by the Joint Armor/Anti-Armor Program through the Advanced Technology Assessment Center at Los Alamos National Laboratory.

We thank John Ramsay for his many contributions to this effort. Joseph Rocchio and Joseph Heimerl of the U.S. Army Ballistic Research Laboratory were essential sources of support. Jacques Charest and Chris Lynch of Dynasen, Inc. performed the gas gun experiments and made many helpful suggestions. Michael Holder and Gilbert Miranda contributed ideas related to the circuit design and analysis, and Bill Wilson of the Naval Surface Warfare Center suggested the form of the calibration equations.

[1] H. C. Vantine, L. M. Erickson, and J. A. Janzen, J. Appl. Phys. **51**, 1957 (1980).
[2] R. W. Watson, Rev. Sci. Instrum. **38**, 978 (1967).
[3] J. Stankiewicz and R. L. White, Rev. Sci. Instrum. **42**, 1067 (1971).
[4] J. L. Austing, A. J. Tullis, and C. D. Johnson, *Proc. 5th Symp. (Int.) on Detonation*, Pasadena, CA, August 18–21, 1970 (Office of Naval Research—Department of the Navy, Arlington, VA, ACR-184-1972), pp. 47–57.
[5] F. Scholz, "Uber die Druckbeeinflussung von Sprengladungen durch die Schwaden fruher detonierender Nachbarladungen beim Sprengen mit Millsekundenzudern im Karbongestein," Ber. Versuchs mbH, Heft 16, Versuchsgruben Gessellschaft mbH, Dortmund, FRG (1981).
[6] K. Hollenberg, "Druckmessungen an Stosswellen in Flussigkeiten und Festkorpen," Der Mathematisch-Naturwissenschaftlichen Fakultat der Universitat Dusseldorf als Habilitationsschrift vergelegt (June 1983).
[7] K. Hollenberg, Propellants, Explosives, Pyrotechnics **11**, 155 (1986).
[8] K. J. Graham, H. P. Richter, C. D. Lind, and A. H. Lepie, *Proc. 1985 JANNAF Propulsion Systems Hazards Subcommittee Meeting*, NASA-Marshall Space Flight Center, Huntsville, AL, 1987 (Chemical Propulsion Information Agency, Laurel, MD, CPIA Publication, 1985), Vol. 1, p. 145.
[9] A. L. Bowman and S. C. Summer, Los Alamos National Laboratory document LA-UR-88-891 (1988).
[10] B. W Asay, A. W. Campbell, M. J. Ginsberg, and J. B. Ramsay, *Proc. 9th Symp. (Int.) on Detonation*, Portland, Oregon, August 27–September 1, 1989 (Office of the Chief of Naval Research, Arlington, Virginia, OCNR 113299-7, 1991), pp. 537–544.
[11] J. A. Charest, Dynasen, Inc., Goleta, CA (unpublished, July 1983).
[12] J. Gregory Glenn, Air Force Armaments Laboratory, FL (unpublished, 1990).
[13] B. W Asay and M. J. Ginsberg, *Proc. 21st Int. ICT Ann. Conf.* (Karlsruhe, Germany, 1990).
[14] K. K. Kuo, B. B. Moore, and V. Yang, *Proc. 16th JANNAF Combustion Meeting*, 1979 (Chemical Propulsion Information Agency, Laurel, Maryland, CPIA Publication 308, 1979), Vol. 1, pp. 559–581.
[15] P. J. Coyne and W. L. Elban, *Proc. Am. Phys. Soc. Topical Conference on Shock Waves in Condensed Matter* Santa Fe, New Mexico, 1983 (North Holland, The Netherlands, 1983), pp. 147–150.
[16] A. B. Anderson, M. J. Ginsberg, W. L. Seitz, and J. Wackerle, *Proc. 7th Symp. (Int.) on Detonation*, Annapolis, Maryland, June 16–19, 1981 (Naval Surface Weapons Center, Dahlgren, Virginia, 1983, NSWC MP 82-334), pp. 385–393.
[17] R. L. Spaulding, Jr., *Proc. 7th Symp. (Int.) on Detonation*, Annapolis, Maryland, June 16–19, 1981 (Naval Surface Weapons Center, Dahlgren, Virginia, 1983, NSWC MP 82-334), pp. 877–886.
[18] B. C. Taylor and L. W. Ervin, *Proc. 6th Symp. (Int.) on Detonation*, Coronado, California, August 24–27, 1976, (Office of Naval Research—Department of the Navy, Arlington, Virginia, ACR-221, 1978), pp. 3–10.
[19] W. M. Wilson, D. C. Holloway, and G. Bjarnholt, *Techniques and Theory of Stress Wave Measurements for Shock Wave Applications* (American Society of Mechanical Engineers, New York, 1987), pp. 97–108.
[20] E. Barsis, E. Williams, and C. Skoog, J. Appl. Phys. **41**, 5155 (1970).
[21] D. E. Grady and M. J. Ginsberg, J. Appl. Phys. **48**, 2179 (1977).
[22] Y. M. Gupta, J. Appl. Phys. **54**, 6094 (1983).
[23] Y. M. Gupta, J. Appl. Phys. **54**, 6256 (1983).
[24] Z. Rosenberg and Y. Partom, *Techniques and Theory of Stress Wave Measurements for Shock Wave Applications* (American Society of Mechanical Engineers, New York, 1987), pp. 133–140.